Optim Eng
DOI 10.1007/s11081-010-9117-z

Practical optimization of group piles using discrete Lagrange multiplier method

Jin-Hung Hwang · Ming-Chien Chung · Der-Shin Juang · Yu-Da Lyu · C. Hsein Juang

Received: 9 June 2008 / Accepted: 8 August 2010

Abstract This paper presents a practical methodology for designing group piles of a bridge foundation that can minimize the construction cost. The constraint functions for the designed pile group are constructed according to the design code currently adopted in local engineering practice. A new procedure based on the discrete Lagrange multiplier (DLM) method is proposed for searching the optimal solution. Seven real-world design cases are used to test the validity and the performance of the proposed procedure and algorithm, in which the DLM solutions are compared with the global optimum solutions obtained by the exhaustive searching method (ESM). Vast improvement in the computational efficiency is achieved, as the DLM method can find local minimum solutions in less than 2.0 to 4.0 minutes whereas the time required with the ESM is 10,000 to 25,000 times longer. In the case studies presented, the construction costs in conjunction with the use of the DLM method differ from the global minimum costs by less than 6.0%, but the savings over the original designs can be as high as 13% to 56%.

Keywords Group pile design · Bridge pier foundation · Practical design · Code based design · Discrete Lagrange multiplier method

J.-H. Hwang (✉) · D.-S. Juang · Y.-D. Lyu
Department of Civil Engineering, National Central University, No. 300, Jhongda Rd, Jhong-li, Taoyuan 32001, Taiwan, China
e-mail: hwangjin@ncu.edu.tw

M.-C. Chung
SINOTECH Engineering Consultants Inc., No. 171, Nanking East Rd., Section 5, Taipei, Taiwan, ROC

C.H. Juang
Department of Civil Engineering, Clemson University, Clemson, SC, USA

Published online: 26 August 2010

1 Introduction

Pile foundations are the most common type of foundations used for bridges located in soft ground or river sites where there are bearing capacity and/or scouring concerns. At a given site, the construction cost of a pile group mainly depends on its layout, including the pile length, diameter, spacing, number, cap and reinforcement of the piles. When the number of the pile group is large, the foundation cost becomes a significant part of the overall project cost. For example, 75% of the structures along the 345 km-long Taiwan High Speed Railway (THSR) are viaducts with bored pile groups. In that project, the number of piles exceeds 30,000, with pile diameter ranging from 1.5 m to 2.5 m and pile length ranging from 50 m to 60 m. The high construction cost for these pile foundations highlights the need for a more cost-effective solution.

Currently, the pile foundation design is based mainly on the trial-and-error procedure as shown in Fig. 1. As shown in the figure, engineers usually adopt an initial design, including the layout and dimensions of piles and cap, according to their own experience and site conditions. Then check whether the design satisfies the code requirements, such as allowable bearing capacities, allowable deformations and rebar reinforcements for piles and cap. After several trials, an acceptable design can generally be established, which will be the final design. The procedure is quite effective, but often produces an overly conservative design. Furthermore, in recent years many large construction projects have been built with the so-called Build-Operate-Transfer (BOT) contracts. With BOT mode, it is essential to optimize the design to achieve the goal of being safer and cheaper; only the design that is optimized with respect to both safety and economy can be most competitive in the current construction market.

The purpose of this paper is to present a code-based optimization algorithm for designing pile groups as a foundation of a bridge that can minimize the construction cost of the foundation. Of course, many factors, both technical and non-technical, can affect the cost of a piled foundation. In this paper, the optimization is limited to the design aspect of a pile group.

Over the past decades, many optimization algorithms have been developed for various engineering problems such as structural design, transportation planning and so forth. However, limited research effort has been directed to the design of pile foundation. Chow and Thevendran (1987) used pile length as the design variable to minimize the difference in bearing loads between the piles in the group. Hoback and Truman (1993) used the optimality criteria (OC) method in conjunction with the branch-and-bound method to conduct least weight designs for a steel pile group. Hurd and Truman (2006) introduced a weightless optimality rule into the original OC approach to treat design variables (such as the spacing and battering of the piles) that have no measurable effect on the objective function. In their study, they only used sectional size and battering angle as design variables. Huang and Hinduja (1986) adopted a quasi-Newton method to optimize the shape of a pile foundation with the assumption of a linear force-deflection relationship for the pile-soil system. Valliappan et al. (1999) applied the generalized reduced gradient method to design pile foundation with the lowest material cost. Their design variables included pile length, diameter,

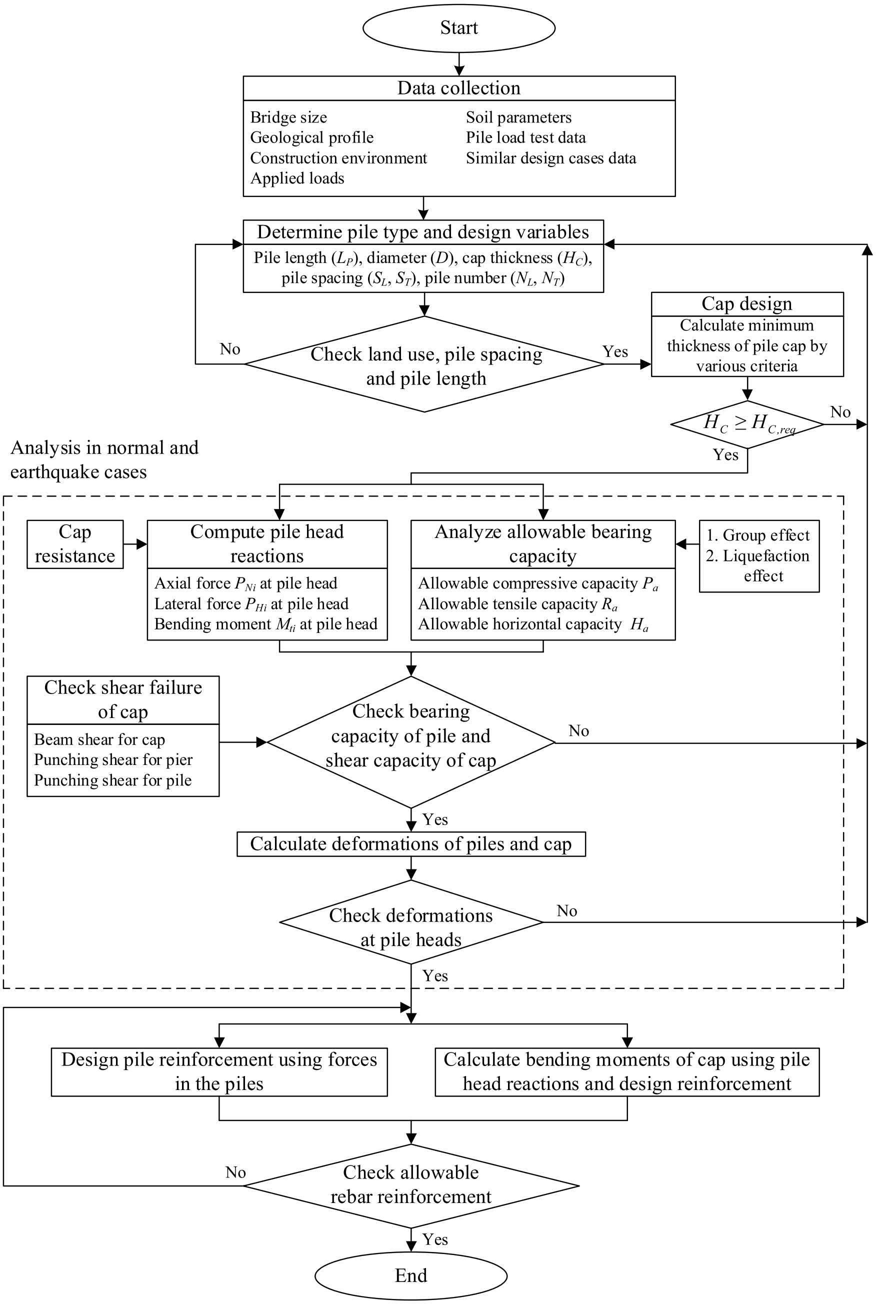

Fig. 1 Trial and error procedure for the design of pile foundation

number and cap. Kim et al. (2001, 2002) used recursive quadratic programming and genetic algorithm to optimize the layout of a pile foundation, with minimum differential settlement being the objective and with the assumption of linear pile-soil interaction. Ng et al. (2005) also adopted a genetic algorithm to optimize the in-situ bored pile foundation groups using the total volume of pile concrete as the objective function without considering steel reinforcement. Chan et al. (2009) presented a hybrid genetic algorithm for pile group foundation design with the concrete volume of the piles and the cap as the objective function.

All the above research has contributed to solving the optimization problems for pile foundation design. However, most of these methods are difficult to apply in practice owing to the fact that the adopted design method and constraints are not code-based and the objective function is not the total construction cost of the pile foundation system. In this paper, a practical method is developed for optimizing pile foundation using the code-based constraints and with the objective of minimizing the construction cost. Here the basis of the optimization algorithm is the discrete Lagrange multiplier (DLM) method, a discrete local search method that has a sound mathematical basis and clear physical meaning. This is an efficient algorithm, as the local minimum solutions can generally be found within 5 minutes for each of the cases studied. To check the accuracy of the DLM, an exhaustive search procedure that can find the true optima for the cases studied is also employed. To implements this procedure, a computer program is developed, which is used to find the true optima for the cases studied. The results of the verification study clearly demonstrate that the proposed DLM algorithm can yield local minimum solutions with high efficiency.

2 Analysis of pile foundation

The response of pile foundations under the action of applied loads can be analyzed with numerical methods such as finite element method (FEM) or simplified method. In this study, a simplified analysis method proposed by Japan Road Association (2002b) is adopted. The simplified method (or model) by Japan Road Association (2002b) can be illustrated with Fig. 2. In this model, the pile cap is assumed to be a rigid plate. The deformations of the cap can be determined using the following equation:

$$\begin{bmatrix} A_{xx} & A_{xy} & A_{x\alpha} \\ A_{yx} & A_{yy} & A_{y\alpha} \\ A_{\alpha x} & A_{\alpha y} & A_{\alpha\alpha} \end{bmatrix} \begin{bmatrix} \delta_x \\ \delta_x \\ \alpha \end{bmatrix} = \begin{bmatrix} H_0 \\ V_0 \\ M_0 \end{bmatrix}, \tag{1}$$

where δ_x, δ_y, and α are the horizontal, vertical and rocking angular displacements of the rigid cap, respectively; H_0, V_0 and M_0 are the horizontal and vertical forces and the moment applied at the center of the cap bottom, respectively. The elements of the coefficient matrix can be calculated as follows:

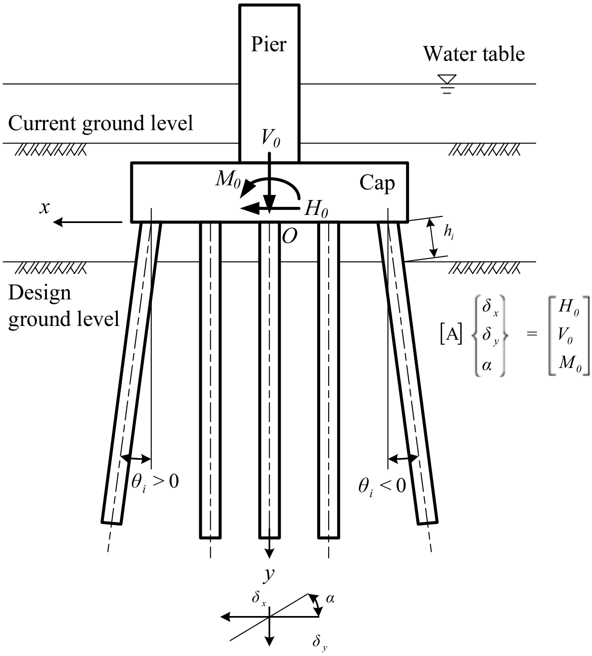

Fig. 2 Analysis model of the pile foundation examined

$$
\begin{aligned}
A_{xx} &= \sum (K_1 \cos^2\theta_i + K_V \sin^2\theta_i),\\
A_{xy} = A_{yx} &= \sum (K_V - K_1)\cos\theta_i \sin\theta_i,\\
A_{x\alpha} = A_{\alpha x} &= \sum \{(K_V - K_1)x_i \sin\theta_i \cos\theta_i - K_2 \cos\theta_i\},\\
A_{yy} &= \sum (K_V \cos^2\theta_i + K_1 \sin^2\theta_i),\\
A_{y\alpha} = A_{\alpha y} &= \sum \{(K_V \cos^2\theta_i + K_1 \sin^2\theta_i)x_i + K_2 \sin\theta_i\},\\
A_{\alpha\alpha} &= \sum \{(K_V \cos^2\theta_i + K_1 \sin^2\theta_i)x_i^2 + (K_2 + K_3)x_i \sin\theta_i + K_4\},
\end{aligned}
\tag{2}
$$

where K_V is the axial stiffness coefficient of the pile head; K_1, K_2, K_3 and K_4 are the other spring coefficients at the pile head. For details of these parameters and their derivation, the reader is referred to Japan Road Association (2002b).

After the deformation of the pile cap is solved, the displacements (δ'_{xi} and δ'_{yi}) and the forces (P_{Ni}, P_{Hi} and M_{ti}) at the head of the ith pile can be determined as follows:

$$
\begin{aligned}
\delta'_{xi} &= \delta_x \cos\theta_i - (\delta_y + \alpha x_i)\sin\theta_i,\\
\delta'_{yi} &= \delta_x \sin\theta_i + (\delta_x + \alpha x_i)\cos\theta_i,\\
P_{Ni} &= K_V \delta'_{yi},\\
P_{Hi} &= K_1 \delta'_{xi} - K_2\alpha,\\
M_{ti} &= -K_3 \delta'_{xi} + K_4\alpha.
\end{aligned}
\tag{3}
$$

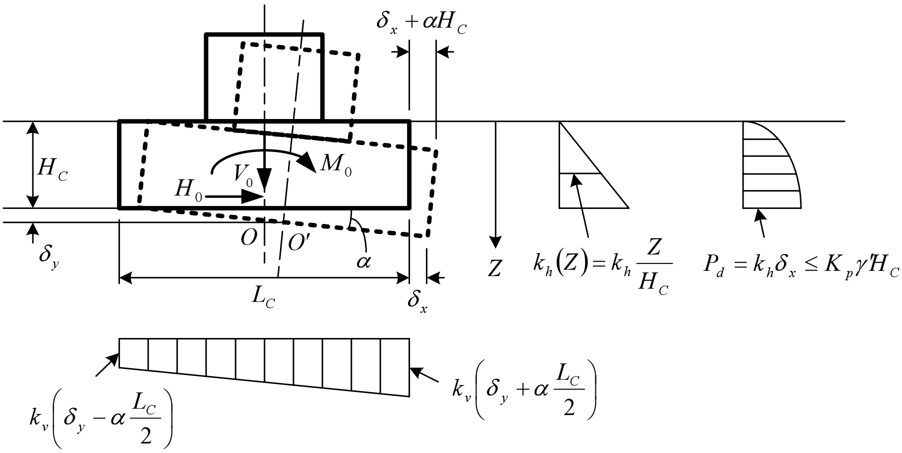

Fig. 3 Resistances at the sides and the bottom of the pile cap

The resistance of the pile cap is also considered in this paper. In reference to Fig. 3, the lateral resistance, H', and moment resistance, M', at the side of the cap can be derived as follows:

$$H' = B_C k_h \left(\frac{1}{2} H_C \delta_x + \frac{1}{6} H_C^2 \alpha \right),$$
$$M' = B_C k_h \left(\frac{1}{6} H_C^2 \delta_x + \frac{1}{12} H_C^3 \alpha \right), \quad (4)$$

where B_C is the width of the cap, k_h is the coefficient of the subground reaction in the horizontal direction within the depth range of the cap, and H_C is the thickness of the cap. The lateral resistance H'', the vertical resistance V'' and the moment resistance M'' at the bottom of the cap can be derived as follows:

$$H'' = k_v B_C L_C f \delta_y,$$
$$V'' = k_v B_C L_C \delta_y,$$
$$M'' = k_v I_b \alpha, \quad (5)$$
$$I_b = \left(\frac{B_C L_C^3}{12} - \sum_{i=1}^{n} A x_i^2 \right),$$

where k_v is the coefficient of the subground reaction in the vertical direction within the range of the cap, L_C is the cap length along the lateral direction, and f is the friction along the interface of the cap bottom and the foundation soil.

To take into account of the effect of the cap, (2) should be rewritten as:

$$
\begin{aligned}
A_{xx} &= \sum \left(K_1 \cos^2\theta_i + K_V \sin^2\theta_i\right) + \frac{1}{2} k_h B_C H_C, \\
A_{xy} &= \sum (K_V - K_1) \cos\theta_i \sin\theta_i + k_v B_C L_C f, \\
A_{x\alpha} &= \sum \{(K_V - K_1) x_i \sin\theta_i \cos\theta_i - K_2 \cos\theta_i\} + \frac{1}{6} k_h B_C H_C^2, \\
A_{yx} &= \sum (K_V - K_i) \cos\theta_i \sin\theta_i, \\
A_{yy} &= \sum \left(K_V \cos^2\theta_i + K_1 \sin^2\theta_i\right) + k_v B_C L_C, \\
A_{y\alpha} &= \sum \left\{\left(K_V \cos^2\theta_i + K_1 \sin^2\theta_i\right) x_i + K_2 \sin\theta_i\right\}, \\
A_{\alpha x} &= \sum \{(K_V - K_1) x_i \sin\theta_i \cos\theta_i - K_2 \cos\theta_i\} + \frac{1}{6} k_h B_C H_C^2, \\
A_{\alpha y} &= \sum \left\{\left(K_V \cos^2\theta_i + K_1 \sin^2\theta_i\right) x_i + K_2 \sin\theta_i\right\}, \\
A_{\alpha\alpha} &= \sum \left\{\left(K_V \cos^2\theta_i + K_1 \sin^2\theta_i\right) x_i^2 + (K_2 + K_3) x_i \sin\theta_i + K_4\right\} \\
&\quad + \frac{1}{12} k_h B_C H_C^3 + k_v I_b.
\end{aligned}
\tag{6}
$$

3 Optimization formulation

3.1 Design variables

The objective of this study was to develop a practical optimization algorithm for the design of pile foundation with a minimum construction cost. As an example to illustrate the methodology, a pile foundation, layout as shown in Fig. 4, is analyzed with two assumptions. One is that these piles have the same diameter and length, and the other is that piles are arranged with a rectangular and symmetrical pattern as shown in Fig. 4. Consequently, the design variables include pile length (L_p), pile diameter (D), thickness of the pile cap (H_C), pile spacing (S_T, S_L), and number of pile (N_T, N_L) in the directions transverse to and longitudinal to the bridge axis. Except for pile numbers (N_T, N_L), all other variables assume real values. Additional symbols are used in Fig. 4 to represent foundation size, applied force, and their directions.

Selection of the design variables has to comply with some limitations, such as the usable land area, the maximum pile length due to piling capability and the pile spacing in relation to excessive grouping and possible construction problems.

3.2 Objective function

The objective function, $F(\boldsymbol{X})$, for the pile foundation design is expressed as the total construction cost of the foundation:

$$F(\boldsymbol{X}) = F_1(\boldsymbol{X}) + F_2(\boldsymbol{X}) + F_3(\boldsymbol{X}) + F_4(\boldsymbol{X}), \tag{7}$$

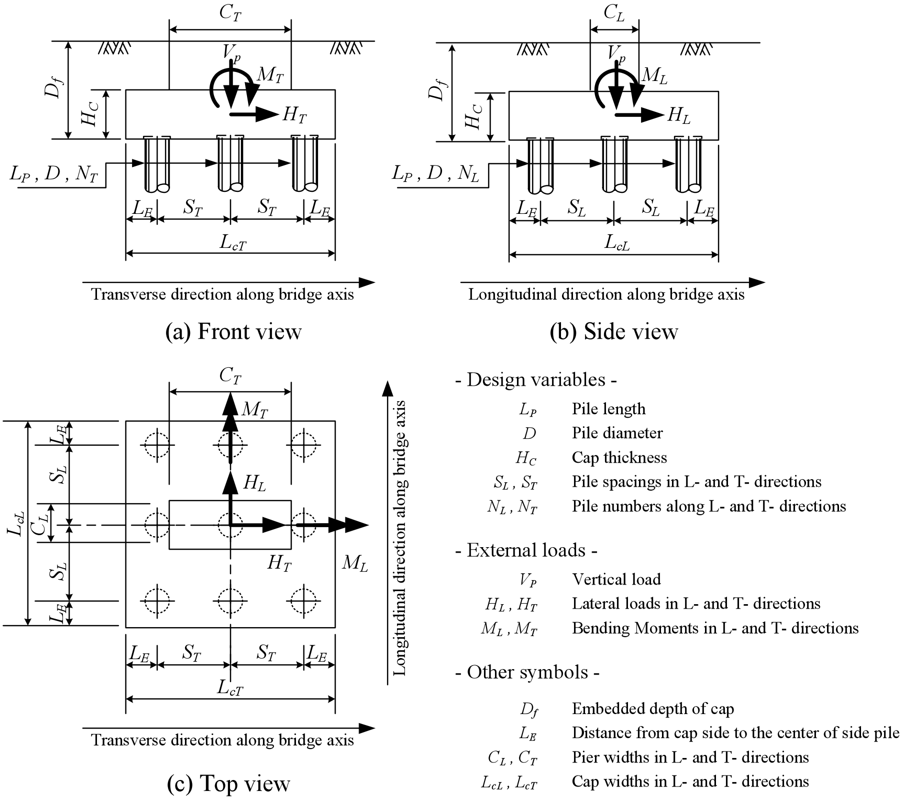

Fig. 4 Symbols for the studied piled foundation

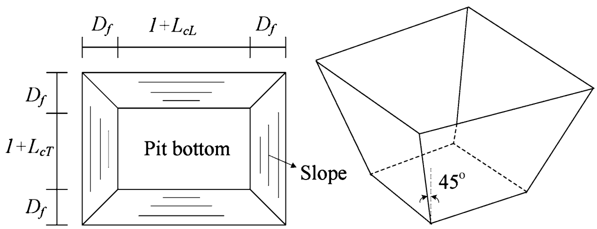

Fig. 5 Schematic diagram showing earth excavation

in which $\boldsymbol{X}$ is a vector of design variables, $F_1(\boldsymbol{X})$ is the excavation cost of the foundation pit, $F_2(\boldsymbol{X})$ is the cost of all piles, $F_3(\boldsymbol{X})$ is the cost of the pile cap, and $F_4(\boldsymbol{X})$ is the cost of backfilling the foundation pit. The details of these items are described below.

3.2.1 Cost of the excavation and backfilling

The excavation cost is $F_1(\boldsymbol{X}) = V_{cut} f_1$, where V_{cut} (m^3) is the volume of the excavation and f_1 (NTD/m^3) is the unit price of earth excavation. Figure 5 shows a schematic diagram of the foundation pit. The pit is excavated from the ground level

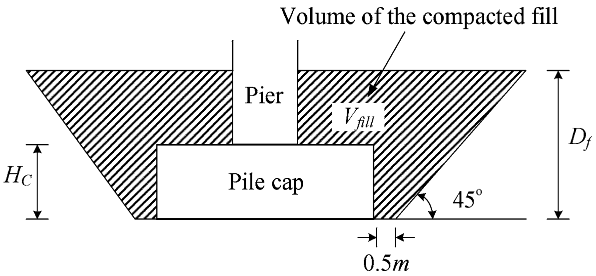

Fig. 6 Schematic diagram showing the volume of compacted fill

to the bottom of the cap with a slope angle of 45°. The excavation bottom is the area of the cap plus 1 m on both sides for the working space. Thus, the volume of the excavation can be computed as:

$$V_{cut} = \frac{4}{3}D_f^3 + (1 + L_{cL})(1 + L_{cT})D_f + D_f^2(1 + L_{cT}) + D_f^2(1 + L_{cL}), \tag{8}$$

where L_{cL} and L_{cT} are the widths of the pile cap in the longitudinal and transverse directions, respectively; D_f is the embedded depth of the pile cap.

The backfill cost is $F_4 = V_{fill} f_6$, where V_{fill} (m^3) is the volume of the compacted backfill as shown in Fig. 6; and f_6 is the unit price of the compacted backfill.

3.2.2 *Cost of the piles and pile cap*

The cost of the piles consists of the costs for concrete, rebars, and pile installation. It may be written as:

$$F_2(\boldsymbol{X}) = N_L N_T (V_{pc} f_2 + V_{ps}\gamma_s f_3 + L_P f_4), \tag{9}$$

where V_{pc} (m^3) is the volume of concrete in the piles; V_{ps} (m^3) is the volume of steel in the piles; γ_s is the unit weight of the rebar; f_2 (NTD/m^3) is the unit price of the concrete; f_3 (NTD/ton) is the unit price of the rebar; and f_4 (NTD/m) is the unit price of the pile installation. The cost of the pile cap includes the material costs for concrete and rebar, and the cost of the formwork for casting the cap. It may be expressed as:

$$F_3(\boldsymbol{X}) = A_{cap} f_5 + V_{cc} f_2 + V_{cs}\gamma_s f_3, \tag{10}$$

where A_{cap} (m^2) is the area of the formwork; V_{cc} (m^3) is the concrete volume for the cap; V_{cs} is the steel volume for the cap; and f_5 (NTD/m^2) is the unit price for installing the formwork.

Note that the required reinforcement (steels) for each set of design variables are specified according to the Design Code and Commentary for Concrete Engineering in Taiwan (The Chinese Institute of Civil and Hydraulic Engineering 2005) which is a modified local version of the ACI code (318-02). The design procedure will be described in Sect. 5.

3.3 Constraints

The constraints for the designed pile foundation are specified according to the design code for bridge foundations published by the Japan Road Association (2002b), supplemented by the Taiwan Reinforced Concrete Design Codes (The Chinese Institute of Civil and Hydraulic Engineering 2005). Totally, six types of constraints are considered in this study. They are described in detail below.

3.3.1 Restriction of usable land

The size of the pile cap and the excavation must be smaller than the area of land available for construction. This constraint may be expressed as:

$$g_1(X) = \frac{(N_i - 1)S_i + 2(D + D_f + 1)}{(L_{ci})_u} - 1 \leq 0, \tag{11}$$

where N_i and S_i are the number of piles and the pile spacing in direction i, respectively, and $(L_{ci})_u$ is the upper limit for the cap size in direction i.

3.3.2 Limitation of pile spacing

According to Japan Road Association (2002b), the minimum pile spacing in each direction has to be greater than the larger one of 0.75 m and 2.5 times the pile diameter. This constraint may be written as

$$g_2(X) = \frac{\max(0.75, 2.5D)}{S_i} - 1 \leq 0. \tag{12}$$

3.3.3 Restriction of pile length

The pile length is restricted by the construction capability of the piling machine. Assuming that the maximum pile length the machine can install is $(L_P)_u$, the constraint may be expressed as

$$g_3(X) = \frac{L_P}{(L_P)_u} - 1 \leq 0. \tag{13}$$

3.3.4 Limitation on the thickness of pile cap

The minimum cap thickness is determined by the following three criteria: (1) the rigidity requirement of the pile cap, (2) the requirements for resisting punching shear and beam shear, and (3) the connection type between pile and cap. The formulas for determining the required minimum cap thickness ($H_{C,req}$) are listed in Table 1. The derivation of these formulas is lengthy; the reader is referred to Chung (2006) for details. The resulting constraint may be written as

$$g_4(X) = \frac{H_{C,req}}{H_C} - 1 \leq 0. \tag{14}$$

Table 1 Formulae for determining cap thickness

Type of pile	Type of pile head connection		Cap thickness for punching shear requirement		Cap thickness for rigidity requirements
	Pile head embedded into the cap	Connection using extended reinforcement into the cap	Working stress method	Ultimate strength method	
Bored pile	–	$H_C \geq 0.1 + 35d_b + D/2$	Punching shear for pier	Punching shear for pier	$H_C \geq \sqrt[3]{\frac{3K_V N_L N_T \bar{\lambda}^4}{L_{cL} L_{cT} E_c}}$
Steel pipe pile	$H_C \geq \frac{\sqrt{D^2 + \frac{4P_{V,\max}}{\pi[8.5+(f_c'-210)/60]}}+D}{2}$		$H_{CE} \geq \frac{\sqrt{(C_L+C_T)^2+\frac{4V_P'}{0.53\sqrt{f_c'}}}-(C_L+C_T)}{4}$	$H_{CE} \geq \frac{\sqrt{(C_L+C_T)^2+\frac{4V_P'}{0.85\times 1.06\sqrt{f_c'}}}-(C_L+C_T)}{4}$	
Prestressed High Strength Concrete pile (PHC pile)	$H_C \geq \max(D+h, 50t+h)$ $h = \frac{\sqrt{D^2 + \frac{4P_{V,\max}}{\pi[8.5+(f_c'-210)/60]}}-D}{2}$		Punching shear for side pile $H_{CE} \geq \frac{\sqrt{D^2+\frac{4P_{V,\max}}{0.53\pi\sqrt{f_c'}}}-D}{2}$	Punching shear for side pile $H_{CE} \geq \frac{\sqrt{D^2+\frac{4P_{V,\max}}{0.85\times 1.06\pi\sqrt{f_c'}}}-D}{2}$	
			Beam shear	Beam shear	
Precast Reinforced Concrete pile (RC pile)	$H_C \geq \frac{\sqrt{D^2 + \frac{4P_{V,\max}}{\pi[8.5+(f_c'-210)/60]}}+D}{2}$		$H_{CE} \geq \frac{q_c \max(L_{cL}-C_L, L_{cT}-C_T)}{2(q_c+0.292\sqrt{f_c'})}$ $H_C = H_{CE}+$ thickness of protecting layer	$H_{CE} \geq \frac{q_c \max(L_{cL}-C_L, L_{cT}-C_T)}{2(q_c+0.85\times 0.53\sqrt{f_c'})}$ $H_C = H_{CE}+$ thickness of protecting layer	

Note: H_{CE}: effective cap thickness (m); E_c: young's modulus of cap concrete (kN/m^2); K_V: spring coefficient at pile head (kN/m); d_b: diameter of rebar (m); f_c': compressive strength of concrete (kgf/cm^2); $\bar{\lambda}$: cantilever length of pile cap (m); t: thickness of hollow PHC pile (m); $P_{V,\max}$: maximum compressive load of pile (kN); q_c: vertical surcharge on the cap (kN/m^2); V_P: external vertical load (kN); $V_P' = V_P(\frac{\text{total number of piles} - \text{pile number under the pier}}{\text{total number of piles}})$; $q_c = \frac{V_P}{L_{cL} L_{cT}}$; C_L, C_T: pier dimensions in longitudinal and transverse directions (m)

3.3.5 Bearing capacity requirements

The compressive, lateral and tensile forces (P_N, P_H, and R_N) applied to the pile head must be less than the allowable compressive, lateral and tensile bearing capacities (P_a, H_a and R_a) for the pile.

The allowable compressive bearing capacity of a single pile may be expressed as

$$P_a = \frac{\sum_i f_{si} A_{pi} + q_b A_b}{FS}, \tag{15}$$

where A_{pi} and A_b are the side perimeter area of the ith pile segment and the area of the pile base, respectively; f_{si} is the unit friction along the ith pile perimeter; q_b is the unit bearing capacity of the pile base; FS is the factor of safety, which is 3.0 for normal loading case (combined action of dead load and live load) and 2.0 for earthquake loading case (combined action of dead load, live load and design earthquake load).

The formulas for calculating the unit friction and end bearing for different types of pile are shown in Tables 2 and 3. In these tables, N is the penetration blow count in a standard penetration test (SPT); c and q_u are the cohesion and uniaxial compressive strength of cohesive soil, respectively.

The allowable lateral bearing capacity, H_a, of a single pile is defined as the lateral load capacity which produces a lateral pile head displacement of 1.5 cm or one percent (1%) of the pile diameter, whichever is larger one. Assuming the pile head is fixed into the pile cap and using Chang's method (1937), the allowable horizontal bearing capacity, H_a, corresponding to the allowable lateral displacement, δ_a, may be derived as

$$H_a = 4EI\beta^3\delta_a, \tag{16}$$

where $\beta = \sqrt[4]{k_h D/(4EI)}$ is the characteristic value of the lateral pile, EI is the flexural rigidity of the pile, and k_h is the coefficient of the horizontal ground reaction.

Table 2 Formulae for estimating unit friction, f_{si} of the pile shaft (Unit: kN/m^2)

Soil type	Bored pile	Steel pipe pile	Driven and pre-bored piles
Sandy and gravelly soils	$5N \leq 200$	$2N \leq 100$	$2N \leq 100$
Clayey soil	c or $10N \leq 150$	c or $10N \leq 150$	$0.8c$ or $8N \leq 100$

Table 3 Formulae for estimating unit end bearing capacity, q_b of the pile base (Unit: kN/m^2)

Soil type	Bored pile	Steel pipe pile	Driven and pre-bored piles
Sandy soil	$100N \leq 3000$	$60D_bN \leq 12{,}000$	$(100 + 40D_b)N \leq 12{,}000$
Gravelly soil	$100N \leq 5000$	$60D_bN \leq 12{,}000$	$(100 + 40D_b)N \leq 12{,}000$
Clayey soil	$3q_u$ or $36N$	$60D_bN \leq 12{,}000$	$(100 + 40D_b)N \leq 12{,}000$

Note: D_b is the ratio of pile penetration depth into the bearing layer to pile diameter

The following empirical equation for k_h was suggested by Japan Road Association (2002b):

$$k_h = 0.34(\alpha_h E_0)^{1.10} D^{-0.31} (EI)^{-0.103}, \tag{17}$$

where α_h is a constant of 1.0 for normal loading case or 2.0 for earthquake loading case, and E_0 is the deformation modulus of the ground which may be estimated from the empirical formula, $E_0 = 28N$.

The allowable tensile bearing capacity, R_a, of a single pile is calculated by

$$R_a = W_P + \frac{1}{FS} \sum_i f_{si} A_{pi}, \tag{18}$$

where W_P is the self weight of a single pile; FS is the minimum safety factor, which is 6.0 for normal loading case and 3.0 for earthquake loading case. Consequently, the bearing capacity constraints may be written as

$$\begin{aligned} g_{5-1}(X) &= \frac{P_N}{P_a} - 1 \le 0, \\ g_{5-2}(X) &= \frac{P_H}{H_a} - 1 \le 0, \\ g_{5-3}(X) &= \frac{R_N}{R_a} - 1 \le 0. \end{aligned} \tag{19}$$

Note that the group effect of a pile foundation and the effect of soil liquefaction during earthquakes on the bearing capacity are also considered in this study. The group effect of a pile foundation is taken into account through the use of two group efficiency factors, η_v and η_h, for the axial and lateral loading directions, respectively. Hanna et al. (2004) have presented the formulas for η_v. Additionally, based on the concept of stress superposition, Yang and Han (1997) proposed a formula considering pile spacing, pile length, pile number, and propagating angle of stress. After a comparison study of these formulas, Yang and Han's formula is adopted here, since their results are more comparable to the field data. The lateral group effect has been studied in detail by Liu (1992) using a large quantity of model pile test results. He proposed an empirical formula for η_h which considers the geometrical parameters of the pile layout, the rigidity of the pile-cap connection, and the resistances of the pile cap. In this study, Liu's formula is adopted for its completeness. The reader is referred to Liu (1992) for details of his formulation.

The bearing capacity and stiffness of a pile foundation is reduced by soil liquefaction during an earthquake. According to Japan Road Association (2002b), this softening effect can be accounted for by a liquefaction reduction factor, D_E, which depends on the safety factor, F_L, against liquefaction, as shown in Table 4. The liquefaction potential of foundation soil can be assessed by the JRA method (Japan Road Association 2002b).

3.3.6 Constraint on lateral displacement of the pile head

According to Japan Road Association (2002b), the allowable lateral displacement, δ_a, at the pile head is equal to 1.0 cm for normal loading case and $0.01D$ for earthquake

Table 4 Reduction factor D_E for soil modulus and strength due to liquefaction effect (Japan Road Association 2002b)

Safety factor against liquefaction	Depth below ground surface z (m)	Cyclic resistance ratio R			
		$R \leq 0.3$		$0.3 < R$	
		Level 1 earthquake	Level 2 earthquake	Level 1 earthquake	Level 2 earthquake
$F_L \leq 1/3$	$0 < z \leq 10$	1/6	0	1/3	1/6
	$10 < z \leq 20$	2/3	1/3	2/3	1/3
$1/3 < F_L \leq 2/3$	$0 < z \leq 10$	2/3	1/3	1	2/3
	$10 < z \leq 20$	1	2/3	1	2/3
$2/3 < F_L \leq 1$	$0 < z \leq 10$	1	2/3	1	1
	$10 < z \leq 20$	1	1	1	1

loading case (when $D \leq 1.5$ m, $\delta_a = 1.5$ cm). This constraint may be written as

$$g_6(X) = \frac{\delta}{\delta_a} - 1 \leq 0. \tag{20}$$

4 Discrete Lagrange multiplier method

In this paper, since all the design variables are discrete, the discrete Lagrangian method (DLM) is adopted to search for discrete optimal solution. The DLM is a discrete version of the Lagrange multiplier method for continuous problems (Shang and Wah 1998). The method has a sound theoretical basis, which yields a constrained local minimum (CLM) in a discrete space. In the following, the formulation and searching procedure of the method are described.

4.1 Weighted discrete Lagrange function

Shang and Wah (1998) defined a discrete Lagrange function (DLF) as follows:

$$DLF = F(\boldsymbol{X}) + \sum_{j=1}^{n_g} \lambda_j H(g_j(\boldsymbol{X})), \tag{21}$$

where λ_j is the Lagrange multiplier corresponding to the jth constraint, n_g is the number of constraints, and H is a transfer function. According to Wu (1998), if the transfer function $H(g_j(\boldsymbol{X}))$ is non-negative, all CLMs have to be a discrete saddle point (DSP), which is defined later. Therefore, $H(g_j(\boldsymbol{X}))$ may be defined in the following as a discrete optimization problem:

$$H(g_j(\boldsymbol{X})) = \max(0, g_j(\boldsymbol{X})), \quad j = 1 \sim n_g. \tag{22}$$

Wu (1998) further proposed that a weighting factor, w, is applied to the objective function as a way to control the solution quality and the speed of convergence. Thus, the weighted DLF may be written as

$$L_d(\boldsymbol{X},\boldsymbol{\lambda}) = wF(\boldsymbol{X}) + \sum_{j=1}^{n_g} \boldsymbol{\lambda}_j H(g_j(\boldsymbol{X})). \tag{23}$$

In this study, the following formula is used to determine the weighting factor based on the findings of Chung (2006):

$$w = \begin{cases} 1.0, & \boldsymbol{X}^{(0)} \in \text{feasible region}, \\ \frac{\max_{j=1}^{n_g} H(g_j(\boldsymbol{X}^{(0)}))}{F(\boldsymbol{X}^{(0)})}, & \boldsymbol{X}^{(0)} \notin \text{feasible region}, \end{cases} \tag{24}$$

in which $\boldsymbol{X}^{(0)}$ is the set of initial design variables selected by the designer. Note that the weighting factor is influenced by the ratio of the constraint value to the objective value. In a feasible region, the value of the transfer functions H for all constraints is zero, therefore, setting $w = 1.0$ can equate the discrete Lagrange function to the objective function, $L_d = F(\boldsymbol{X})$.

4.2 Discrete saddle point

A discrete saddle point (DSP) is defined as follows. For all possible $\boldsymbol{\lambda}$'s that are sufficiently close to $\boldsymbol{\lambda}^*$, and for any $\boldsymbol{X}$ within the neighborhood of $\boldsymbol{X}^*$, the point $(\boldsymbol{X}^*, \boldsymbol{\lambda}^*)$ is a DSP if the following relations hold:

$$L_d(\boldsymbol{X}^*,\boldsymbol{\lambda}) \le L_d(\boldsymbol{X}^*,\boldsymbol{\lambda}^*) \le L_d(\boldsymbol{X},\boldsymbol{\lambda}^*). \tag{25}$$

For minimization problems with constraints of $g_j(\boldsymbol{X}) \le 0$, the corresponding $\boldsymbol{\lambda}_j$ must be non-negative. Since $\boldsymbol{\lambda}_j \ge 0$, the first inequality relation of (25) holds only if $H(g_j(\boldsymbol{X}^*)) = 0$ is satisfied. This means that $\boldsymbol{X}^*$ must be a feasible solution. The second inequality relation implies that $\boldsymbol{X}^*$ is a minimum point for $\boldsymbol{\lambda} = \boldsymbol{\lambda}^*$. Consequently, a DSP must also be a CLM for the problem examined.

In reference to Wu (1998), the discrete gradient of the weighted DLF at a point $\boldsymbol{X}$ for a fixed set of Lagrange multipliers $\boldsymbol{\lambda}$ can be defined as:

$$\Delta_x L_d(\boldsymbol{X},\boldsymbol{\lambda}) = \boldsymbol{Y} - \boldsymbol{X}, \tag{26}$$

where $\boldsymbol{Y}$ is the design point with the minimum value of L_d for all the design points in the set $\boldsymbol{X} \cup N(\boldsymbol{X})$. Obviously, if the point $\boldsymbol{X}^*$ is a CLM, then the following two conditions must be satisfied:

$$\Delta_X L_d(\boldsymbol{X}^*,\boldsymbol{\lambda}^*) = 0, \tag{27}$$

$$\nabla_{\lambda_j} L_d(\boldsymbol{X}^*,\boldsymbol{\lambda}^*) = H(g_j(\boldsymbol{X}^*)) = 0, \quad j = 1 \sim n_g. \tag{28}$$

4.3 Neighborhood

In this paper, the set of neighborhood, $N(\boldsymbol{X})$, for the design variables, $\boldsymbol{X}$, is defined as

$$N(\boldsymbol{X}) = \bigcup_{i=1}^{m} \bigcup_{j=1}^{b_i} (x_1, \ldots, x_{i-1}, x_i \pm (\Delta x_i)_j, x_{i+1}, \ldots, x_m) \tag{29}$$

in which m is the number of design variables; $x_i - (\Delta x_i)_j$ and $x_i + (\Delta x_i)_j$ are the jth neighboring points below and above x_i, respectively. The parameter b_i is the number of discrete points below and above the current design variable, x_i. In this paper, the initial value of b_i is set to be one.

4.4 First-order searching formula

To find a DSP, which is equivalent to search for a CLM in a discrete design space, the following two equations are proposed (Steps 10 in Fig. 7):

$$\boldsymbol{X}^{(s+1)} = \boldsymbol{X}^{(s)} + \Delta_X L_d(\boldsymbol{X}^{(s)}, \boldsymbol{\lambda}^{(s)}), \tag{30}$$

$$\boldsymbol{\lambda}_j^{(s+1)} = \boldsymbol{\lambda}_j^{(s)} + C \frac{H(g_j(\boldsymbol{X}^{(s+1)}))}{\max_{j=1}^{n_g} H(g_j(\boldsymbol{X}^{(s+1)}))}, \quad \text{for } \max_{j=1}^{n_g} H(g_j(\boldsymbol{X}^{(s+1)})) > 0, \tag{31}$$

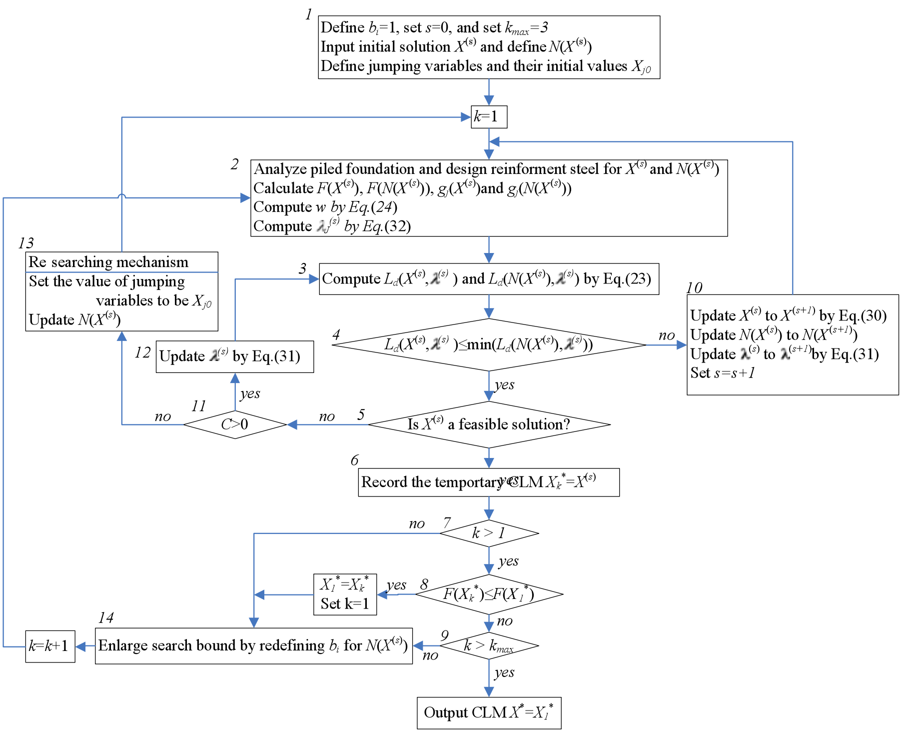

Fig. 7 Flow chart for the DLM algorithm

where s is the number of iterations, and C is a positive real number for controlling the updated speed of $\boldsymbol{\lambda}$.

According to (30), the search will move along the discrete gradient direction of the L_d at $\boldsymbol{X}^{(s)}$. Concurrently, the Lagrange multipliers are increased by using (31) to penalize the violated constraints until a DSP is reached.

Since the ratio of objective value to the sum of the violated constraint values can be adjusted by selecting an appropriate weight parameter w in (24), the following initial $\boldsymbol{\lambda}_j^{(0)}$ for different constraints is proposed in this paper:

$$\boldsymbol{\lambda}_j^{(0)} = \frac{H(g_j(\boldsymbol{X}^{(0)}))}{\max_{j=1}^{n_g} H(g_j(\boldsymbol{X}^{(0)}))}. \tag{32}$$

In (31), an appropriate value of C should be determined such that at least one of $L_d(N(\boldsymbol{X}), \boldsymbol{\lambda}^{(s+1)})$ is smaller than $L_d(\boldsymbol{X}, \boldsymbol{\lambda}^{(s+1)})$ once the Lagrange multipliers are updated from $\boldsymbol{\lambda}^{(s)}$ to $\boldsymbol{\lambda}^{(s+1)}$. A formula for determining the value of C is provided by Chung (2006):

$$C = \min\left(\frac{L_d(N_i(\boldsymbol{X}^{(s+1)}), \boldsymbol{\lambda}^{(s)}) - L_d(\boldsymbol{X}^{(s+1)}, \boldsymbol{\lambda}^{(s)})}{(\delta L_d)_X - (\delta L_d)_{Ni}}\right), \tag{33}$$

where $N_i(\boldsymbol{X}^{(s+1)})$ is the ith neighboring point in the set $N(\boldsymbol{X}^{(s+1)})$; $(\delta L_d)_X = \sum_{j=1}^{n_g} \Delta\boldsymbol{\lambda}_j H(g_j(\boldsymbol{X}^{(s+1)}))$; $(\delta L_d)_{Ni} = \sum_{j=1}^{n_g} \Delta\boldsymbol{\lambda}_j H(g_j(N_i(\boldsymbol{X}^{(s+1)})))$; $\Delta\boldsymbol{\lambda}_j = H(g_j(\boldsymbol{X}^{(s+1)}))/\max_{k=1}^{n_g} H(g_k(\boldsymbol{X}^{(s+1)}))$. One should note that the value of C must be positive to ensure that there exists at least one of $N(\boldsymbol{X}^{(s+1)})$ as a valid candidate of CLM for the next movement. When C is negative, it implies that $\boldsymbol{X}^{(s)}$ has already reached the valley of a local convex region in the design space. In this case, if $\boldsymbol{X}^{(s)}$ is feasible, it will be a valid CLM. Otherwise, an enhanced search technique, as described in the next section, has to be used to help the search escape from the local convex region.

4.5 Enhanced techniques for the DLM

Since the DLM is a local search method, in a pile foundation design problem, which is a multimodal problem, the search may be trapped in a local convex region in either feasible or infeasible domain. To overcome this drawback, two enhanced techniques are adopted to help the search escape from a local convex region.

The first enhanced technique is to widen the search range by redefining the set $N(\boldsymbol{X})$ to include more neighboring points after a CLM has been found (Step 14 in Fig. 7). Based on the results of a sensitivity study, a range of five points neighboring the current CLM is suggested for variables (L_P, S_L, S_T), three points for variables (D, H_C) and two points for variables (N_L, N_T).

Widening the search range does not alter the characteristics of a local searching procedure. To assure better solution quality, a re-searching mechanism that forces the search point to jump out of the infeasible region where it is trapped to start a new search, or to jump out of a CLM to search for a better CLM, is also adopted. The idea is to select several design variables as jump-out variables x_j (Step 13 in Fig. 7) and set their values to the initial values $x_j^{(0)}$, while maintaining the other design variables unchanged. Using $x_j^{(0)}$ as an initial solution, the DLM searching process is repeated. If the re-searched CLM is better than the previous one, it replaces the previous CLM. The re-searching procedure will be terminated when the objective value can no longer be reduced further after $k_{\max}$ times of re-search (Step 9 in Fig. 7). In this study, $k_{\max}$ was set to 2.

5 Design of steel reinforcements

For each set of design variables, $\boldsymbol{X}$ and $N(\boldsymbol{X})$, the required steel reinforcements for piles and pile cap must be designed according to the requirements of the Design Code and Commentary to Concrete Engineering in Taiwan (The Chinese Institute of Civil and Hydraulic Engineering 2005), in reference to Step 2 in Fig. 7. The step-by-step procedures for steel reinforcement design are described below:

1. Consider all possible design combinations incorporating different bar sizes and spacing that are commonly used in engineering practice.
2. Check whether these combinations satisfy the code requirements regarding the reinforcement ratio, bar spacing and stress restrictions. Choose the design that requires the minimum quantity of rebar from those that satisfy the code requirements.
3. If no combination satisfies the code requirements, the pile diameter or the cap size is probably too small. The size must be adjusted to form new design alternatives and the above procedures are repeated until an optimal steel reinforcement design can be obtained.

Each pile is divided into three segments, according to steel reinforcements. The first segment is from the pile head to the depth with half of the maximum bending moment, $M_{\max}/2$. The second segment is from the depth of $M_{\max}/2$ to the depth with minimum moment capacity, $M_{\min}$, corresponding to the minimum steel bar area, $A_{i,\min}$, required by the code. The third segment is from the depth of $M_{\min}$ to the bottom of the pile. The reinforcement of the pile cap is designed considering punching shear, beam shear and moment requirements for the critical sections. The rebars required for negative and positive bending moments are arranged on the lower and upper sides of the cap. The rebars required on each side should be arranged in three layers at most.

6 Case studies and performance of the DLM

In this section, six real design cases will be used to assess the performance of the DLM. Among them, cases I and II are cases of pile foundation designs for highway bridges. Cases III through VII are for Taiwan high speed railway (THSR) bridges. Cases selected cover different geological and loading conditions. Only Case I is described in detail herein due to space limit.

In order to understand the conservativeness of a design, a safety surplus index (SSI) is defined in this paper. The SSI for the ith stress or deformation state is defined below,

$$S_i = \left(1 - \frac{V_{d,i}}{V_{all,i}}\right) \times 100\%, \tag{34}$$

where $V_{d,i}$ is the ith analyzed variable state, such as the force and displacement of the pile head; $V_{all,i}$ is the allowable value of the ith variable state required by code, such as the allowable bearing capacity and lateral displacement. The index SSI denotes the "normalized" difference between the analyzed variable and the allowable value. The analyzed ith state is safe if $S_i \geq 0$. However, if $S_i < 0$, the unsafe condition prevails in the ith state, which implies that the design is controlled by the ith variable state. In this paper, eight S_i indices are introduced. They are S_1 for checking compressive bearing capacity of the pile; S_2 for tensile bearing capacity of the pile; S_3 for compressive bearing capacity of the pile group; S_4 for lateral bearing capacity of the pile group; S_5 for lateral displacement of the pile head; S_6 for the punching shear check of the bridge pier; S_7 for the punching shear check of a side pile; and S_8 for checking the beam shear.

6.1 Comparison between the exhaustive searching method (ESM) solution and the original design

This case discusses a bored pile foundation design for a highway bridge across a river in eastern Taiwan. The design load combination is shown in Table 5. The peak ground acceleration is 0.22 g. Figure 8 shows the geological profile while the soil parameters are shown in Table 6. The profile shows an upper sandy layer of 20 m, underlain by a gravel layer with a thickness of over 40 m. The safety factors and unit prices used in the design are shown in Tables 7 and 8. The lower and upper bounds for the design variables used in ESM and DLM searches are 15 m $\leq L_P \leq$ 30 m, 3.5 m $\leq S_L, S_T \leq$ 7 m, 1.5 m $\leq D \leq$ 2 m, 3 m $\leq H_C \leq$ 4 m, and $3 \leq N_L, N_T \leq 6$, respectively. The step sizes for the design variables are set to $(L_P, S_L, S_T, D, H_C, N_L, N_T) =$ (0.1 m, 0.1 m, 0.1 m, 0.1 m, 0.1 m, 1, 1).

Table 9 shows the original design solution and the global solution found by the ESM. Figure 9 displays a breakdown of the total costs of the original solution and the ESM solution for different items. A personal computer equipped with a 2 GHz CPU and 256 MB of SDRAM is used for design calculation. As shown in Table 9, the ESM search takes 59,720 minutes to find the optimal solution and the number

Table 5 Design loads for the piled foundation for Case I

External loads	Normal case	Earthquake case (combination 1)	Earthquake case (combination 2)
Vertical force V_P (kN)	76,200	132,000	117,000
Horizontal force in L-direction H_L (kN)	2100	50,000	19,500
Horizontal force in T-direction H_T (kN)	5700	9000	39,000
Moment in L-direction M_L (kN m)	18,000	300,000	60,000
Moment in T-direction M_T (kN m)	126,000	99,000	540,000

Fig. 8 Geological profile for Case I

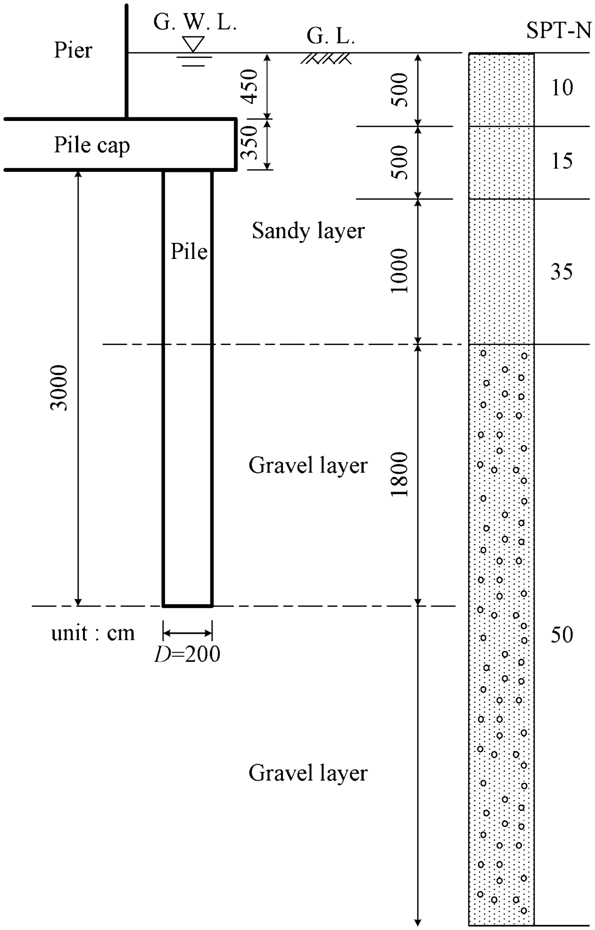

Table 6 Soil parameters used in Case I

Depth (m)	Soil type	SPT-N	Unit weight γ (kN/m^3)	Cohesion c (kN/m^2)	Friction angle ϕ (°)
0.0–5.0	Sandy soil	10	19.0	–	27.0
5.0–10.0	Sandy soil	15	19.5	–	27.0
10.0–20.0	Sandy soil	35	20.0	–	37.5
20.0–60.0	Gravel soil	50	21.0	–	40.0

of pile analyses is 11,943,936 times. The global solution saves 51.3% as compared to the original one. Specifically, the pile length is greatly reduced from the original 30 m to 15 m. The pile diameter is also reduced from 2.0 m to 1.5 m. Similarly, the cap size is reduced from the original size of 22.0 m × 24.0 m × 3.5 m to the size of

Table 7 Safety factors used in Case I

Name of case	Design condition	End bearing capacity	Frictional capacity	Tensile capacity
Case I	Normal case	3	3	6
	Earthquake case	2	2	3

Table 8 Unit prices of construction processes and materials used in Case I

Name	Unit prices
Earth excavation (f_1)	31 NTD/m^3
Concrete (f_2)	1550 NTD/m^3
Steel rebar (f_3)	8100 NTD/ton
Pile construction (f_4) ($D = 1.0$ m)	
Alluvial soil	750 NTD/m
Gravel soils	1125 NTD/m
Soft rock	1688 NTD/m
Framework assembling (f_5)	250 NTD/m^2
Backfill and compaction (f_6)	50 NTD/m^3

Table 9 Comparison of the ESM and the original design solutions for Case I

Design solution	L_p	D	H_C	S_L	S_T	N_L	N_T	Cost (NTD)	Analysis number	Computation time (min)
Original	30	2.0	3.50	6.00	5.00	4	5	13,728,879	–	–
ESM	15	1.5	3.80	4.30	3.80	4	6	6,681,762	11,943,936	59,720.0

Note: The ESM solution saves about 51.3% as compared to the original one

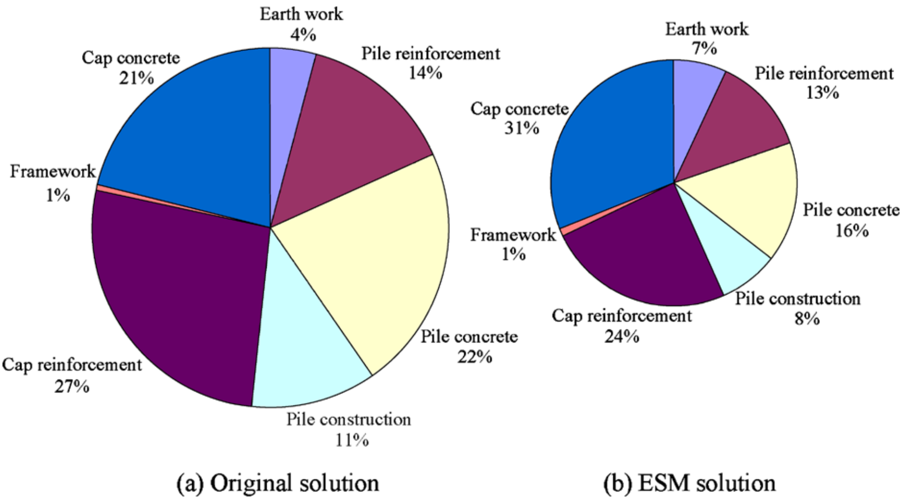

Fig. 9 Cost breakdown for the ESM and the original solutions

Table 10 Pile reinforcements for the ESM and the original solutions for Case I

Design solution		Reinforced segment (m)	Rebar size	Rebar number	Rebar ratio $\rho(\%)$	Reinforcement diagram (section of first segment)
Original	A	0–10	2D32	32	1.66	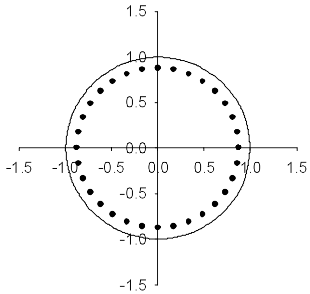
	B	10–30	D32	32	0.83	
	C	–	–	–	–	
ESM	A	0–7	D25	52	1.49	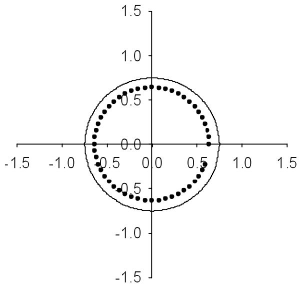
	B	7–15	D25	36	1.03	
	C	–	–	–	–	

Note: A, B and C denote different reinforced segments of the pile. For definitions refer to Fig. 10

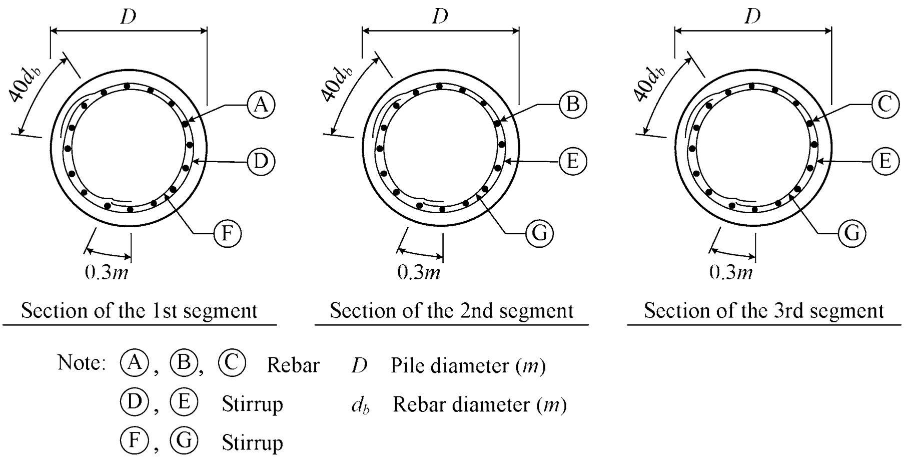

Fig. 10 Schematic diagram showing pile reinforcements for different segments

15.9 m × 22.0 m × 3.8 m. These reductions represent a significant decrease in the costs of concrete, earthwork and formwork.

The ESM pile reinforcement designs and the original solutions are listed in Table 10. Figure 10 shows the pile reinforcements for A, B and C segments described

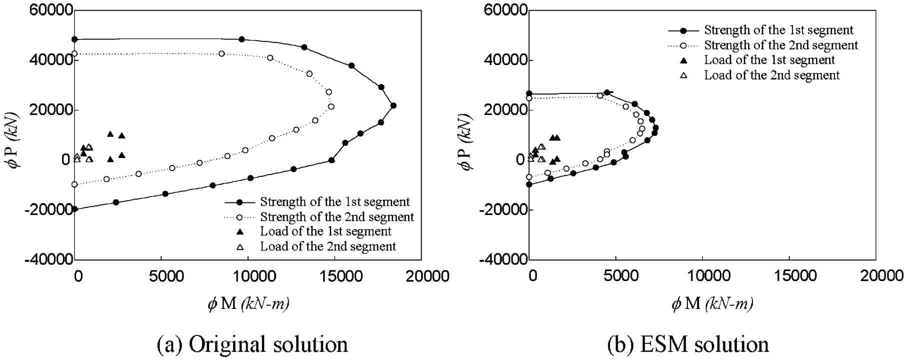

Fig. 11 P-M strength curves and the pile forces for the ESM and the original solutions for Case I

Table 11 Cap reinforcements for the ESM and original solutions for Case I

Position of reinforcement	Direction		Original		ESM	
Upper rebar	Longitudinal	D1	D32@15	1294.3 cm^2	D32@20	895.4 cm^2
	(L direction)	D2	–		–	
		D3	–		–	
	Transverse	B1	D32@15	1188.4 cm^2	D32@15	854.7 cm^2
	(T direction)	B2	–		–	
		B3	–		–	
Lower rebar	Longitudinal	C3	2D36@15	9606.8 cm^2	–	4753.8 cm^2
	(L direction)	C2	2D36@15		2D32@15	
		C1	2D36@15		2D32@15	
	Transverse	A3	2D36@15	8821.3 cm^2	2D36@15	6344.1 cm^2
	(T direction)	A2	2D36@15		2D36@15	
		A1	2D36@15		2D36@15	

Note: A1–A3, B1–B3, C1–C3, D1–D3 denote different reinforcing layers. For definitions refer to Fig. 12

in Table 10. Figure 11 displays the axial force-moment (P-M) capacity curves and design loads of the piles for both solutions. It can be seen that the original reinforcement is conservative as its designed P-M states are far less than the P-M strength curve. Table 11 shows the pile cap reinforcements for the ESM and the original solutions. Figure 12 displays the notations for different reinforcing layers in longitudinal and transverse directions in Table 11. The original reinforcement is nearly twice that of the ESM solution. This proves again that the original design is too conservative.

Figure 13 shows a comparison of all the SSIs in the ESM and original solutions. It can be observed that in six SSIs (S_1, S_2, S_3, S_4, S_5 and S_8), the ESM solutions are lower than those for the original one. This means that the ESM solution is not as conservative as the original one. A comparison of the design variables shows that

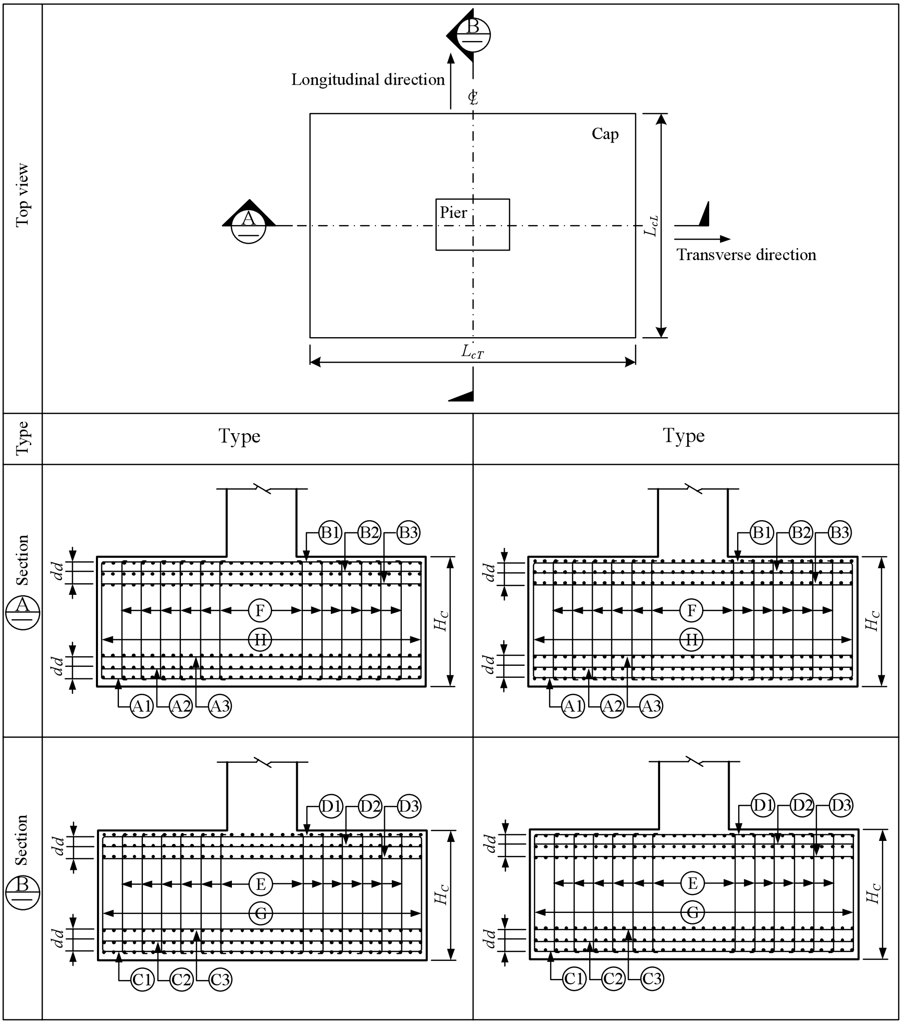

Fig. 12 Schematic diagram showing pile cap reinforcement

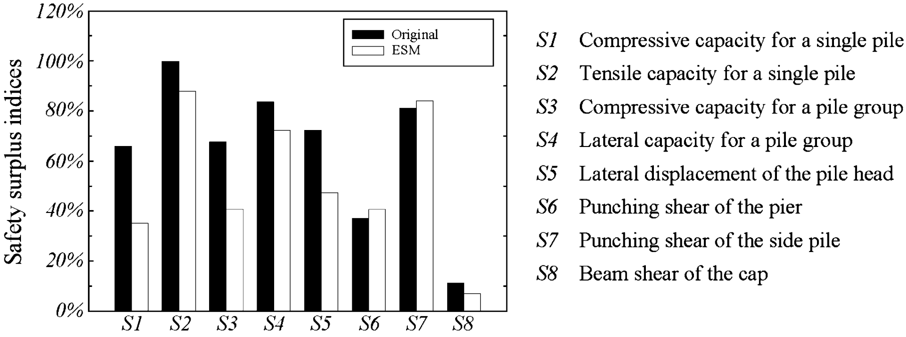

Fig. 13 Safety surplus indices for the ESM and the original solutions for Case I

the original penetration depth into the bearing layer (gravel layer) of 18 m makes the allowable compressive bearing capacities of the pile (15,939 kN for normal loading case; 48,946 kN for earthquake loading case) far higher than the forces caused by design loads (5417 kN for normal loading case; 14,552 kN for earthquake loading case). This appears to be too conservative. In the ESM solution, the penetration depth into the bearing layer is reduced to 3.1 m, which reduces pile length from 30 m to 15 m, and accordingly decreases the allowable compressive bearing capacities to 6,629 kN for normal loading case and 20,422 kN for earthquake loading case. These allowable compressive bearing capacities are still higher than the design loads (4,300 kN for normal loading case; 12,438 kN for earthquake loading case).

The layout of the ESM not only satisfies the safety requirements, but is more economical than the original design. The four SSIs related to the pile bearing capacities in the ESM solution are all reduced to lower values, indicating that the ESM solution is effective in terms of bearing capacity. The horizontal displacement of the pile head in the ESM solution increases from 0.55 cm to 0.79 cm but still satisfies the code requirements.

Table 12 Comparison of ESM and DLM searching results for all cases

Case	Method	L_P	D	H_C	S_L	S_T	N_L	N_T	Cost (NTD)	Number of Analysis	Spending time (min)
Case I	Original	30	20	3.5	6.00	5.00	4	5	13,728,879	–	–
	ESM	15	1.5	3.80	4.30	3.80	4	6	6,681,762	11,943,936	59,720.0
	DLM	15	1.5	3.80	4.30	3.80	4	6	6,681,762	479	2.5
Case II	Original	15	1.2	2.2	3.05	3.05	3	3	2,039,924	–	–
	ESM	26	1.1	1.8	4.10	3.60	2	2	1,391,274	10,221,120	51,100.0
	DLM	26	1.1	1.8	4.15	3.85	2	2	1,414,723	588	3.0
Case III	Original	58	2.0	2.5	9.00	6.00	2	3	7,203,524	–	–
	ESM	25	1.8	2.8	4.50	4.60	4	2	4,541,702	10,349,856	51,750.0
	DLM	25	1.5	2.7	3.80	3.80	4	3	4,679,075	324	2.0
Case IV	Original	58	2.0	2.5	9.00	6.00	2	3	7,203,524	–	–
	ESM	36	1.5	2.6	3.80	3.80	4	3	5,145,433	10,349,856	51,750.0
	DLM	36	1.5	2.6	3.80	3.80	4	3	5,145,433	590	3.0
Case V	Original	52	2.0	2.5	8.00	8.00	2	2	4,614,478	–	–
	ESM	34	1.8	2.9	4.90	5.30	3	2	3,635,136	10,349,856	51,750.0
	DLM	32	1.9	2.9	4.80	4.80	3	2	3,731,428	406	2.5
Case VI	Original	49	2.0	2.5	8.00	8.00	2	2	4,244,042	–	–
	ESM	25	2.0	2.9	5.00	5.00	3	2	3,497,323	10,349,856	51,750.0
	DLM	27	1.9	3.0	5.80	5.60	3	2	3,705,527	662	3.5
Case VII	Original	50	2.0	2.5	8.00	8.00	2	2	4,296,826	–	–
	ESM	26	1.9	2.7	4.80	5.60	3	2	3,293,419	10,349,856	51,750.0
	DLM	26	1.9	2.7	4.80	5.60	3	2	3,293,419	718	5.0

Table 13 DLM searching performance for all Cases

Case name	Saving as compared to the original solution (%)	Difference from ESM (%)	Analysis number	Time Spent (min)
Case I	48.81	0.00	479	2.5
Case II	30.65	1.69	588	3.0
Case III	56.31	2.58	324	2.0
Case IV	28.57	0.00	590	3.0
Case V	19.14	2.65	406	2.5
Case VI	12.69	5.95	662	3.5
Case VII	23.35	0.00	718	5.0
Avg.	31.36	1.86	538	2.9

6.2 Performance of the DLM

Table 12 shows a comparison of the design variables, total cost, number of analyses and computation times for the original, ESM, and DLM solutions for cases I through VII. It can be seen that for cases II, IV and VII, the DLM solutions are the same as the ESM solutions, indicating that the DLM can reach the global minimum solution. Table 13 summarizes the performance of the DLM for these cases. The results show that the DLM can search out local minimum solutions within 2.0 to 5.0 minutes which is only 1/25,875 to 1/10,350 of the time spent by the ESM. The construction cost of the local minimum solution differs from that of the global minimum solution by less than 6.0%, a saving of about 13% to 56% as compared to the original design solution. The performance of the DLM appears to be good enough and its use in the optimization of pile foundation designs is warranted.

7 Concluding remarks

This paper presents a framework where pile foundation design can be optimized for minimizing the total construction costs. The adopted design methodology is *code-based* so that it requires no complicated numerical analysis such as the finite element method. This means that the pile analysis can be completed quickly so that the implementation of the DLM takes only a few minutes, which makes the design methodology quite acceptable in routine designs. Almost all the factors affecting pile design are considered and the constraints are deliberately formulated. The proposed safety surplus indices (SSI) help monitor how close the solution is to the boundaries of various constraints so that engineers can realize what kinds of constraints dominate the design.

A program is developed to perform pile analysis and formulate designs with an optimization module for conducting ESM and DLM searches. For the real case studies discussed in the paper, we demonstrate how reliably the DLM can find the local minimum solutions efficiently with great accuracy (with less than 6% difference from the global minimum solutions). The DLM solutions also save about 13% to 56% in total construction costs, compared to the original design solutions. Thus, this methodology is shown to be a promising tool for solving optimization problems in the applicable geotechnical fields.

Acknowledgements This study was financially supported by the Taiwan National Science Council through Grants NSC92-2622-E-008-007-CC3, NSC93-2622-E-008-006-CC3 and NSC94-2622-E-008-009-CC3. These financial supports by the NSC are greatly appreciated.

References

Chan CM, Zhang LM, Ng JTM (2009) Optimization of pile groups using hybrid genetic algorithms. J Geotech Geoenviron Eng 135(4):497–505

Chang YL (1937) Discussion on lateral pile-loading tests. Trans ASCE 102:272–278

Chow YK, Thevendran V (1987) Optimization of pile groups. Comput Geotech 4(1):43–58

Chung MC (2006) Optimum design of piled foundations. PhD Dissertation, Department of Civil Engineering, National Central University, Jhong-li, Taiwan

Hanna AM, Morcous G, Helmy M (2004) Efficiency of pile groups installed in cohesionless soil using artificial neural networks. Can Geotech J 41(6):1241–1249

Hoback AS, Truman KZ (1993) Least weight design of steel pile foundations. Eng Struct 15(5):379–385

Huang Z, Hinduja S (1986) Shape optimization of a foundation for a large machine tool. Int J Mach Tool Des Res 26(2):85–97

Hurd AJ, Truman KZ (2006) Optimization method of pile foundations. In: Proceedings of an international conference on advances in engineering structures, mechanics & construction, Waterloo, Ontario, Canada, 14–17 May, pp 653–661

Japan Road Association (2002a) Specifications for highway bridges part IV: substructures. Tokyo, Japan

Japan Road Association (2002b) Specifications for highway bridges part V: seismic design. Tokyo, Japan

Kim KN, Lee SH, Kim KS, Chung CK, Kim MM, Lee HS (2001) Optimal pile arrangement for minimizing differential settlements in piled raft foundations. Comput Geotech 28:235–253

Kim HT, Koo HK, Kang IK (2002) Genetic algorithm-based optimum design of piled raft foundations with model tests. J Southeast Asian Geotech Soc 33(1):1–11

Liu JL (1992) The method for calculating the separate synthetic pile group coefficients of lateral bearing capacity. J Soil Rock Eng 14(3):9–19

Ng JTM, Chan CM, Zhang LM (2005) Optimum design of pile groups in nonlinear soil using genetic algorithms. In: Proceedings of the 8th international conference on the application of artificial intelligence to civil, structural and environmental engineering, Rome, Italy, 30 August–2 September, 2005, paper 35. doi:10.4203/ccp.82.35

The Chinese Institute of Civil and Hydraulic Engineering (2005) Design code and commentary to concrete engineering (DCCCE). Scientific & Technical Publishing, Taiwan

Valliappan S, Tandjiria V, Khalili N (1999) Design of raft-pile foundation using combined optimization and finite element approach. Int J Numer Anal Methods Geomech 23(10):1043–1065

Yang KJ, Han LA (1997) Pile engineering. China Communications Press, Beijing, pp 13–77

Shang Y, Wah BW (1998) A discrete Lagrangian-based global search method for solving satisfiability problems. J Glob Optim 12(1):61–99

Wu Z (1998) The discrete Lagrangian theory and its application to solve nonlinear discrete constrain optimization problems. Master Thesis, Department of Computer Science, University of Illinois at Urbana-Champaign